Time Series Modelling - Final Assignment

PhD in Statistical Sciences, University of Bologna

July 15, 2024

Discussion of the paper *"COVID-19 Active Case Forecasts in Latin American Countries Using Score-Driven Models (Contreras-Espinoza et al., 2023)"* with an application to COVID-19 Bologna data

Marika D'Agostini

Contents

1 Introduction

The COVID-19 pandemic has highlighted the need for rapid and accurate computational modelling that provides forecasts to public health authorities on how day-to-day interventions can control the spread of a novel virus. Although many different models have been proposed, score-driven and state-space models represent a class of models that has been particularly fruitful in matching the dynamics of infectious diseases due to their inherent flexibility and robustness. An application of these models is presented in the work *COVID-19 Active Case Forecasts in Latin American Countries Using Score-Driven Models* by Contreras-Espinoza et al. (2023) where score-driven models were used to forecast active COVID-19 cases in multiple Latin American countries.

The first class of time series models for new COVID-19 cases forecasting employed by (Contreras-Espinoza et al., 2023) comprises score-driven models. These are observation-driven state-space models in which the dynamic parameters are observable quantities that are updated every time new information becomes available. In particular, (Contreras-Espinoza et al., 2023) used a score-driven model for the negative binomial distribution, incorporating local-level and trend components. They also further extended it by adding a weekly seasonal component for new COVID-19 cases.

The second set of models used in the paper are state-space models with unobserved components. (Contreras-Espinoza et al., 2023) extended the state-space model by adding a weekly seasonal component, and assuming a negative binomial distribution for the data-generating process which is robust against possible small numbers of newly reported cases. By using the new state-space model with unobserved components for the negative binomial distribution, they separately modelled the trend, seasonality, and seasonal components of new COVID-19 cases, and they studied the forecasting accuracy for new COVID-19 cases using alternative forecasting windows (7, 14 and 28 days).

The main purpose of this project is to discuss the work of Contreras-Espinoza et al., and to apply their research to a new context: the area served by the Bologna wastewater treatment plant (WWTP). This area covers the city of Bologna and its neighbouring municipalities, with a population of approximately 800,000. By applying the score-driven and state-space models to the COVID-19 case data from this region, I aim to assess the performance and adaptability of these models in a different epidemiological and geographical setting.

The rest of this report is organized as follows: Section 2 presents the data, the statistical models and the methodology used to assess statistical performance and forecasting capability; Section 3 presents the results related to the Bologna COVID-19 data; Section 4 presents a discussion of (Contreras-Espinoza et al., 2023); Section 5 presents the conclusions.

2 Materials and Methods

2.1 Study Area and COVID-19 Data

A three-step selection process was carried out to identify the study area. First, the initial boundary of the study area was established as the union of all areas encompassed by or intersecting the catchment area of the sewer network serviced by the main wastewater treatment plant (WWTP) in Bologna. Next, any areas enclosed by the initially selected regions were included. Finally, areas primarily associated with other treatment facilities were excluded from the selection. This process resulted in a study area encompassing nearly all the census sections of Bologna, and a portion of the census sections of the neighbouring municipalities (Figure 1).

Figure 1: Map of the study area (orange), wastewater treatment plant (red triangle), sewer network (blue), catchment area (light blue).

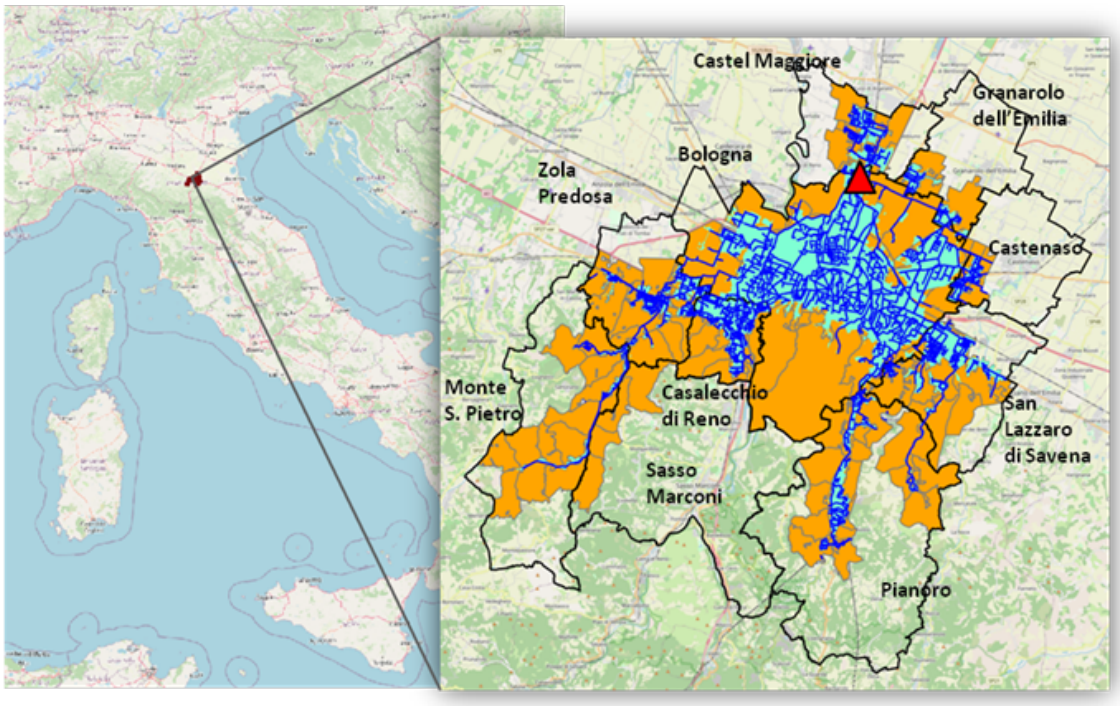

To assess the performance of models described by (Contreras-Espinoza et al., 2023), data on newly reported COVID-19 cases provided by the Local Health Authority of Bologna were used. Specifically, employed data spans from October 13, 2021, to April 4, 2023, covering daily new cases within the WWTP service area. For each confirmed COVID-19 case, further detailed information is also available, including the census area where isolation took place, presence and onset date of symptoms, date of the swab test, diagnosis date, hospital admission and discharge dates, outcome (whether recovery or death), outcome date, and, if applicable, cause of death if applicable.

The time series data used in this project is available in the file `dati.xlsx`.

2.2 Score-Driven Model with Different Seasonality Components (SD1)

In the score-driven models used to predict new COVID-19 cases described in (Contreras-Espinoza et al., 2023),

$$y_t \sim p(y_t|y_1, \ldots, y_{t-1}, f_t, \Theta)$$

where y_t denotes the number of new COVID-19 cases in period t, f_t is the score-driven parameter, and Θ is a vector of constant parameters.

Similar to the work of (Harvey & Kattuman, 2020), the paper of (Contreras-Espinoza et al., 2023) assumes that the data-generating process for new COVID-19 cases is a negative binomial distribution with shape parameter ν, and therefore the conditional density of y_t is defined as

$$p(y_t|y_1, \ldots, y_{t-1}, f_t, \theta) = \frac{\Gamma(\nu + y_t)}{y_t!\,\Gamma(\nu)} \left(\frac{f_t}{\nu + f_t}\right)^{y_t} \left(\frac{\nu}{\nu + f_t}\right)^{\nu} \tag{1}$$

The dynamics of $\ln y_t$ are then formulated as follows:

$$\ln y_t = \delta_t + s_t \tag{2}$$

$$\delta_t = \delta_{t-1} + \beta_{t-1} + \kappa_1 u_{t-1} \tag{3}$$

$$\beta_t = \beta_{t-1} + k_2 u_{t-1} \tag{4}$$

$$s_t = D_t \gamma_t \tag{5}$$

$$D_t = (D_{\text{Monday},t}, \ldots, D_{\text{Sunday},t}) \tag{6}$$

$$\gamma_t = \gamma_{t-1} + \kappa_t u_{t-1} \tag{7}$$

where δ_t (1 × 1) is the local level component, β_t (1 × 1) is the trend component, s_t (1 × 1) is the seasonality component, and γ_t (7 × 1) is a vector of seasonality filter whose elements are defined as

$$\gamma_t = (\gamma_{\text{Monday},t}, \dots, \gamma_{\text{Sunday},t})^T \tag{8}$$

and where κ_t is a (7 × 1) vector with

$$\kappa_{j,t} = \begin{cases} \kappa_j, & \text{if } D_{j,t} = 1 \\ -\dfrac{\kappa_j}{7-1}, & \text{if } D_{j,t} = 0 \end{cases} \quad \text{for} \quad j \in \{\text{Monday}, \dots, \text{Sunday}\}. \tag{9}$$

Hence, in this first Score Driven model (SD1) parameters κ_j are time-invariant.

Finally, following the work of (Harvey & Kattuman, 2020), the scaled score function updating term present in Equations (3), (4) and (7) is given by $u_t = \dfrac{y_t}{f_t} - 1$, which is the score function (i.e., the conditional score of the log-likelihood with respect to f_t) divided by the information quantity.

The functions used to implement the SD1 model in R are available in the `SD1.R` file.

2.3 Score-Driven Model with Equal Seasonality Components (SD2)

The (Contreras-Espinoza et al., 2023) paper also considers alternative specifications of the general score-driven model SD1 described in Section 2.2. The first one (denoted SD2) assumes that all seasonality parameters are identical, i.e., $\kappa_j = \kappa \quad \forall j$.

In the SD2 model, the dynamics of $\ln y_t$ are therefore formulated as follows:

$$\begin{aligned} \ln y_t &= \delta_t + s_t \\ \delta_t &= \delta_{t-1} + \beta_{t-1} + \kappa_1 u_{t-1} \\ \beta_t &= \beta_{t-1} + k_2 u_{t-1} \\ s_t &= D_t \gamma_t \\ D_t &= (D_{\text{Monday},t}, \dots, D_{\text{Sunday},t}) \\ \gamma_t &= \gamma_{t-1} + \kappa u_{t-1} \end{aligned}$$

where δ_t (1 × 1) is the local level component, β_t (1 × 1) is the trend component, s_t (1 × 1) is the seasonality component, and γ_t (7 × 1) is a vector of seasonality filter whose

elements are defined as

$$\gamma_t = \left(\gamma_{\text{Monday},t}, \ldots, \gamma_{\text{Sunday},t}\right)^T.$$

The functions used to implement the SD2 model in R are available in the `SD2.R` file.

2.4 Score-Driven Model without Seasonality Components (SDWS)

The second alternative specification of SD1 presented in (Contreras-Espinoza et al., 2023) assumes that only local-level and trend components are included in the model, i.e., $s_t = 0 \quad \forall t = 1, \ldots, T$. This latter specification is denoted as SDWS (score-driven without seasonality), and the dynamics of $\ln y_t$ are formulated as follows:

$$\begin{aligned}
\ln y_t &= \delta_t + s_t \\
\delta_t &= \delta_{t-1} + \beta_{t-1} + \kappa_1 u_{t-1} \\
\beta_t &= \beta_{t-1} + k_2 u_{t-1}
\end{aligned}$$

where δ_t (1 × 1) is the local level component and β_t (1 × 1) is the trend component.

The functions used to implement the SDWS model in R are available in the `SDWS.R` file.

2.5 State-Space Model (SS)

The fourth model described in (Contreras-Espinoza et al., 2023) is a nonlinear state-space model with unobserved components for the negative binomial distribution, denoted SS. The authors followed the work of (Helske et al., 2021), using the exponential family state-space model and applying it to the negative binomial distribution.

The same conditional density for y_t used for the score-driven models, see Equation (1), was also used in the SS model. In this case, the negative binomial model is approximated by a Gaussian model, and the estimation is performed using the Kalman filter procedure.

The log-mean of y_t is then formulated by Equations (10)–(16):

$$\ln f_t = \delta_t + s_t \tag{10}$$

$$\delta_t = \delta_{t-1} + \beta_{t-1} + \epsilon_{\delta,t} \tag{11}$$

$$\beta_t = \beta_{t-1} + \epsilon_{\beta,t} \tag{12}$$

$$s_t = D_t \gamma_t \tag{13}$$

$$D_t = D_{\text{Monday},t}, \ldots, D_{\text{Sunday},t} \tag{14}$$

$$\gamma_t = \gamma_{t-1} + \epsilon_{\gamma,t} \tag{15}$$

$$\epsilon_{\gamma,t} = (\epsilon_{\text{Monday},t}, \ldots, \epsilon_{\text{Sunday},t}) \tag{16}$$

where δ_t (1 × 1) is the local level component, β_t (1 × 1) is the tend component, s_t (1 × 1) is the seasonality component, and γ_t (7 × 1) is the seasonality filter of time-varying parameters. It was assumed that

$$\epsilon_{\delta,t} \sim N(0, \sigma_\delta^2)$$
$$\epsilon_{\beta,t} \sim N(0, \sigma_\beta^2)$$

and that

$$\epsilon_{\gamma,t} \sim N(0, \sigma_\gamma^2(I_7 - \frac{1}{7} i_7 i_7'))$$

where I_7 is the identity matrix and i_7 is a (7 × 1) vector of ones. In particular, this specification of the covariance matrix of $\epsilon_{\gamma,t}$ ensures that the sum of the seasonality filters is zero in each period.

To proceed with the R implementation, the SS model has been cast into the state-space framework as follows:

1. Observation Equation:

   $$y_t = Z_t \alpha_t + \epsilon_t$$

   with

   $$\alpha_t = \begin{pmatrix} \delta_t \\ \beta_t \\ \gamma_t \end{pmatrix}, \quad Z_t = \begin{pmatrix} 1 & 0 & D_t \end{pmatrix}$$

   where Z_t is the system matrix of the observation equation, considering the structure of α_t.

2. State Equations:

   $$\delta_t = \delta_{t-1} + \beta_{t-1} + \epsilon_{\delta,t}$$
   $$\beta_t = \beta_{t-1} + \epsilon_{\beta,t}$$
   $$\gamma_t = \gamma_{t-1} + \epsilon_{\gamma,t}$$

These can be compactly written as

$$\alpha_t = T_t \alpha_{t-1} + R_t \eta_t$$

with

$$T_t = \begin{pmatrix} 1 & 1 & 0 \\ 0 & 1 & 0 \\ 0 & 0 & I_7 \end{pmatrix}$$

$$R_t = I_9$$

$$\eta_t = \begin{pmatrix} \epsilon_{\delta,t} \\ \epsilon_{\beta,t} \\ \epsilon_{\gamma,t} \end{pmatrix} \sim \mathcal{N}(0, Q_t)$$

$$Q_t = \begin{pmatrix} \sigma^2_\delta & 0 & 0 \\ 0 & \sigma^2_\beta & 0 \\ 0 & 0 & \Sigma_\gamma \end{pmatrix}$$

where T_t is the state transition matrix, R_t is the state disturbance matrix, and η_t is the state disturbance vector assumed to be drawn from a multivariate normal distribution with mean zero and covariance matrix Q_t.

3. Initial State:

$$a_1 = \begin{pmatrix} \delta_1 \\ \beta_1 \\ \gamma_1 \end{pmatrix}, \quad P_1 = \text{cov}(\alpha_1)$$

where a_1 is the initial state vector (assuming it starts at 0) and P_1 is the covariance matrix of the initial state, initialized with some large variance.

The functions used to implement the SS model in R are available in the `SS.R` file.

2.6 Parameter Estimation and Statistical Performance

All models described in Sections 2.2-2.5 are estimated using the maximum likelihood method, in which the following log-likelihood (LL) function is maximized with respect to the parameter vector Θ

$$\hat{\Theta} = \underset{\Theta}{\text{argmax}}\, \text{LL}(y_1, \ldots, y_T, \Theta) = \underset{\Theta}{\text{argmax}} \sum_{t=1}^{T} \ln p(y_t | y_1, \ldots, y_{t-1}, f_t, \Theta).$$

The performance of the different statistical models is compared using the AIC Akaike information criterion (AIC), the corrected AIC (AICc), and the Bayesian Information Criterion (BIC) defined as follows

$$\begin{aligned} \text{AIC} &= 2K - 2\,\hat{\text{LL}} \\ \text{AICc} &= \text{AIC} + \frac{2K(K+1)}{T-K-1} \\ \text{BIC} &= K\ln(T) - 2\,\hat{\text{LL}} \end{aligned}$$

where $\hat{\text{LL}}$ is the maximum value of the log-likelihood, K is the number of estimated time-invariant parameters, and T denotes the sample size, i.e. the length of the time series.

2.7 Prediction Performance

The SD1, SD2, SDWS, and SS forecast precisions are studied for each of the considered prediction windows (7, 14 and 28 days) using the Mean Square Error(MSE), the Mean Absolute Error (MAE) and the Mean Absolute Percentage Error (MAPE), defined as follows

$$\begin{aligned} \text{MSE} &= \frac{1}{T}\sum_{t=1}^{T}(y_t - y_{f,t})^2 \\ \text{MAE} &= \frac{1}{T}\sum_{t=1}^{T}|y_t - y_{f,t}| \\ \text{MAPE} &= \frac{1}{T}\sum_{t=1}^{T}\frac{|y_t - y_{f,t}|}{y_t} \end{aligned}$$

3 Results

To evaluate the in-sample and out-of-sample performances of the models described by (Contreras-Espinoza et al., 2023), a time series of new daily infections of COVID-19 in the area served by the main Bologna WWTP, from October 13, 2021, to April 4, 2023 ($T = 539$ observations) is used.

Table 1 presents the data summary statistics, the p-value of the Jarque–Bera (JB) test (Jarque & Brera, 1980) and the p-value of the augmented Dickey–Fuller (ADF) test (Dickey & Fuller, 1979). For the JB test, the null hypothesis of normal distribution is rejected at the 1% significance level. This supports the use of the negative binomial

distribution for the score-driven model. For the ADF test, the null hypothesis that a unit root is present in the time series cannot be rejected, which supports using the unit root specifications for δ_t in Equations (3) and (11). These results are aligned with those obtained by (Contreras-Espinoza et al., 2023) for nine Latin American countries, justifying the use of the data regarding new daily infections of COVID-19 in the area served by the main Bologna WWTP to evaluate (Contreras-Espinoza et al., 2023) models' performance.

Table 1: Descriptive statistics, JB test, and ADF test for new COVID-19 cases

Mean	**Std. Dev.**	**Minimum**	**Maximum**
354.264	413.413	13	2659

Skewness	**Kurtosis**	**JB *p*-value**	**ADF *p*-value**
2.631	11.139	0.000	0.055

For the full sample period, parameter estimates for SD1, SD2, SDWS, and SS are reported in Table 2. The parameters κ_1 and κ_2 are significant in both SD1, SD2 and SDWS, indicating that the local level (δ_t) and trend (β_t) components are crucial for these models. Moreover, the estimates are relatively consistent, suggesting robustness in capturing the core dynamics of the data.

Looking at the seasonal parameters of SD1 ($\kappa_{j,t}$ where $j \in \{\text{Monday, Tuesday, } \ldots, \text{Sunday}\}$, a significant effect of Mondays emerged. This might capture weekly patterns in reporting case numbers, reflecting some regularity in data collection or transmission cycles. Also κ_{Saturday} and κ_{Sunday} are significant, suggesting a potential weekend effect on the data, likely due to reporting delays. The seasonality parameter κ is also significant for SD2, confirming the presence of a weekly seasonal trend in the data.

The dispersion parameter of the negative binomial distribution (ν) is significant across all models. The values vary widely, with the highest being in the SS model (72.6) and the lowest in the SDWS model (9.30). This indicates different levels of over-dispersion captured by each model.

The variance components of the SS model (σ^2_β, σ^2_γ, σ^2_δ) are all significant. This suggests that the SS model explicitly accounts for additional sources of variability. Even though

Table 2: Parameter estimates

	SD1	**SD2**	**SDWS**	**SS**
κ_1	0.408 *** (0.030)	0.391 *** (0.029)	0.196 *** (0.017)	-
κ_2	0.074 *** (0.010)	0.070 *** (0.010)	0.053 *** (0.006)	-
κ_{Monday}	0.169 *** (0.063)	0.111 *** (0.019)	-	-
κ_{Tuesday}	0.000 (0.000)	-	-	-
$\kappa_{\text{Wednesday}}$	0.000 (0.000)	-	-	-
κ_{Thursday}	0.000 (0.000)	-	-	-
κ_{Friday}	0.000 (0.000)	-	-	-
κ_{Saturday}	0.103 ** (0.041)	-	-	-
κ_{Sunday}	0.228 *** (0.056)	-	-	-
ν	38.2 *** (2.76)	35.3 *** (2.62)	9.30 *** (0.60)	72.6 *** (8.83)
σ^2_β	-	-	-	0.0000 (0.001)
σ^2_δ	-	-	-	0.0002 *** (0.000)
σ^2_γ	-	-	-	0.0001 *** (0.000)

Notes: Standard errors are in parentheses. ***, **, and * indicate parameter significance at the 1%, 5%, and 10% levels, respectively. For SD2, $\kappa_j = \kappa_{\text{Monday},t}$ for $j = \text{Tuesday}, \ldots, \text{Sunday}$.

the estimates are very small, the inclusion of these components could explain the higher ν value and reflect a greater adaptability to data variations.

In Figures 1-4, for each of the four models tested, the filtered estimates of new cases of infection with COVID-19 are represented together with the observed time series. SD1, SD2 and SS appear to have similar performance, with the estimates (red lines) and observed data (black lines) showing close alignment across the time series. Both models show some deviations at the peaks but generally capture the overall trend series well. SDW instead seems to capture only the overall trend of the series, with less accuracy in capturing the sharp fluctuations in the data. This suggests that the SDWS model may not be as reliable in terms of prediction accuracy.

To evaluate the predictive capacity of the SD1 SD2, SDWS and SS models, the same procedure used by (Contreras-Espinoza et al., 2023) was followed. First, the observed time series was divided into two equal parts (270 and 269 observations, since T=539). Considering a 7-day prediction window, the last 7 observations were removed from

Figure 2: Filtered estimates of new cases of infection with COVID-19 (SD1)

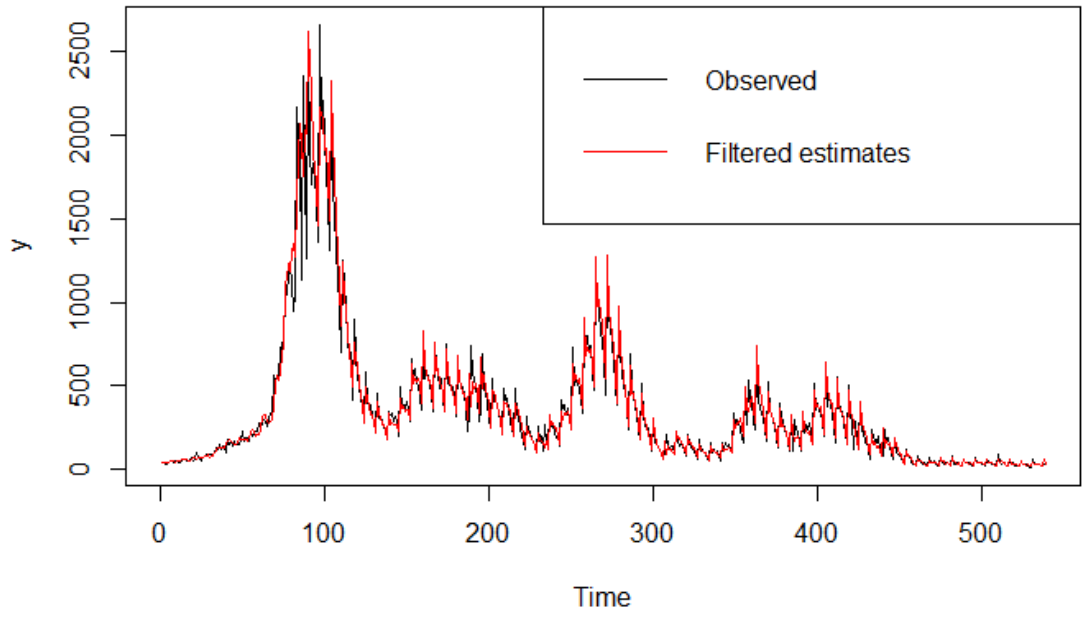

Figure 3: Filtered estimates of new cases of infection with COVID-19 (SD2)

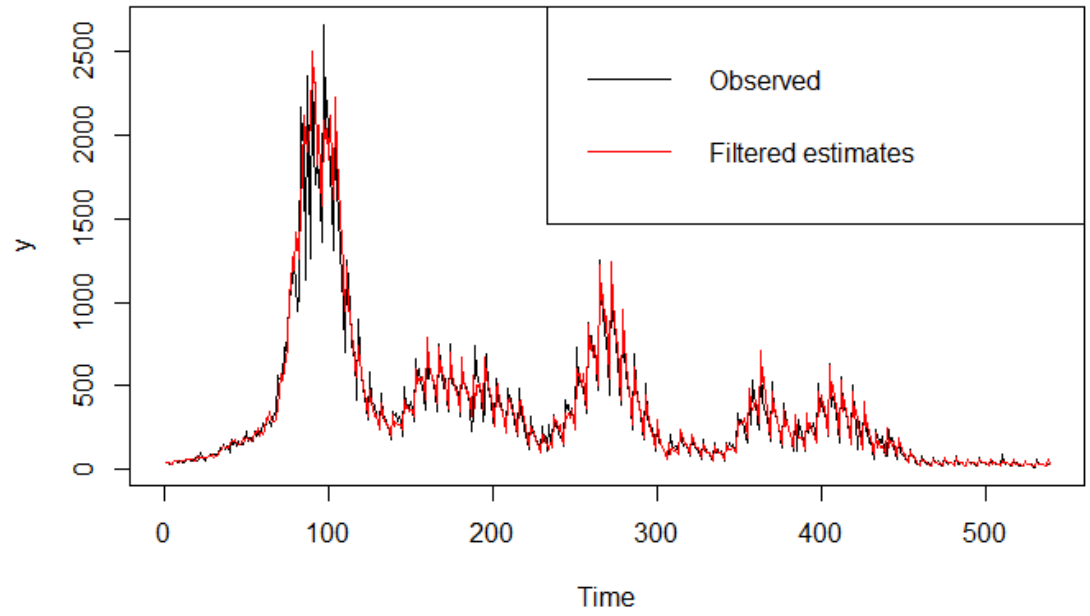

Figure 4: Filtered estimates of new cases of infection with COVID-19 (SDWS)

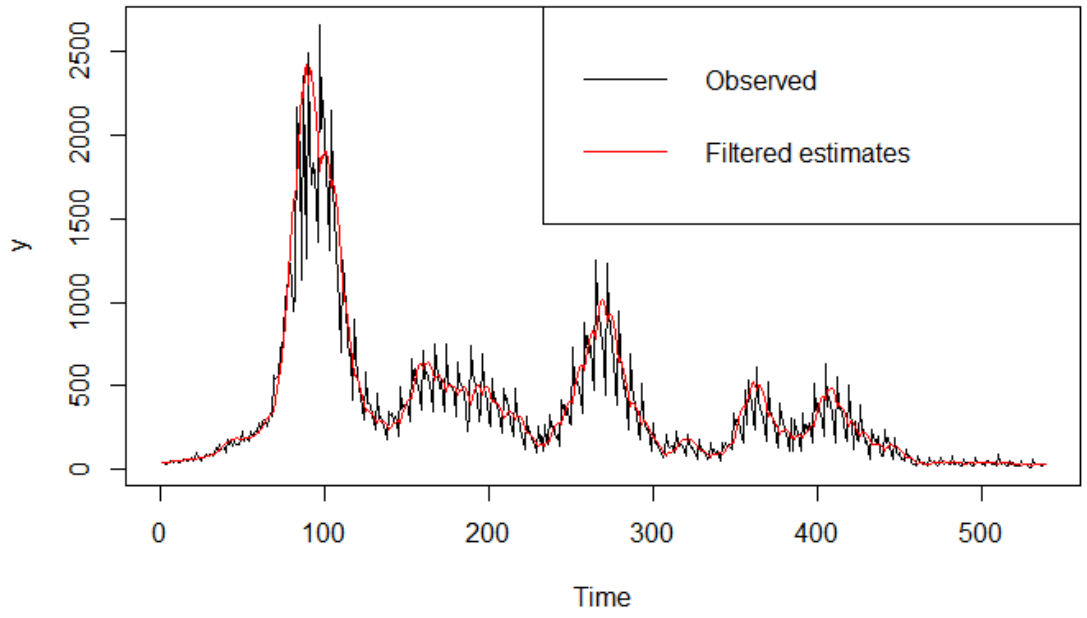

Figure 5: Filtered estimates of new cases of infection with COVID-19 (SS)

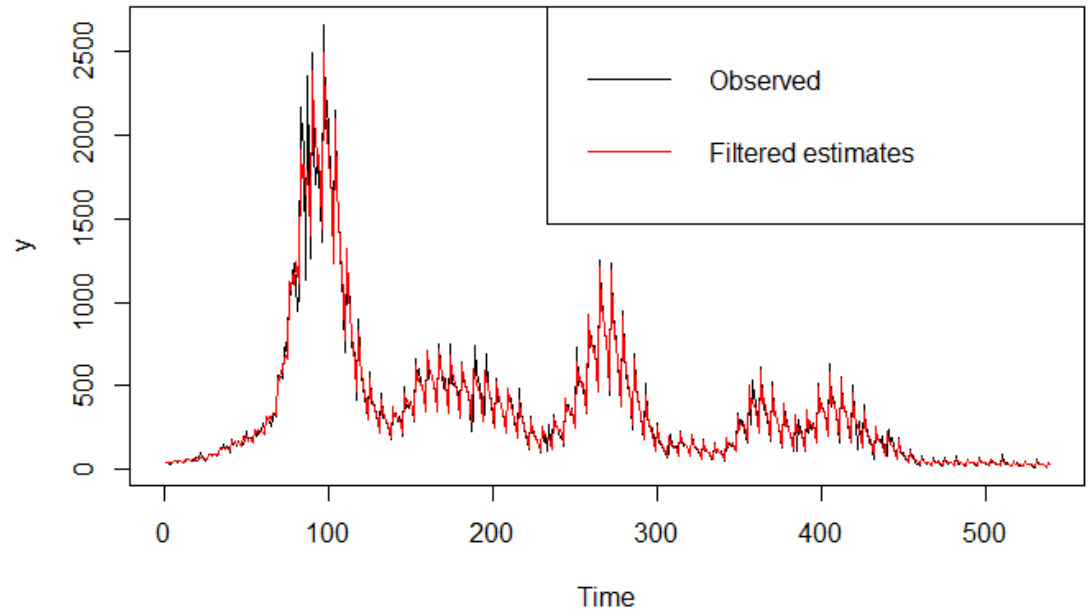

the initial half of the data and predicted using the remaining data and the parameters presented in Table 2. The metrics described in sections 2.6 and 2.7 were calculated to evaluate statistical performance and predictive capacity of the fitted models. Then, the next observation (observation 271) was included in the fitting data. The last 7 observations were again removed and predicted using parameters in Table 2, and the prediction quality was evaluated. These steps were repeated until the total set of available observations was considered. Finally, the same procedure was repeated using 14- and 28-day time windows.

Tables 3, 4 and 5 show the mean values of AIC, AICc, BIC, MSE, MAE, and MAPE for the different models considering 7-, 14- and 28-day estimation windows, respectively. SD2 has the best performance in terms of AIC, AICc and BIC, suggesting it is the best model when it comes to considering the trade-off between model complexity and fit. SD1 has instead the lowest prediction accuracy metrics for all three forecasting windows tested (the best values have been highlighted in bold). SDWS seems to be the least preferred model among those tested due to poorer fit and prediction accuracy. Furthermore, when the size of the forecasting window increases, the prediction quality of all models decreases: for example, the SD1 MAPE value is 22.5% for the 7-day forecast, 34% for the 14-day forecast and 75.54% for the 28-day forecast.

Table 3: AIC, AICc, BIC, and loss functions (forecasting window: 7 days)

Model	**AIC**	**AICc**	**BIC**	**MSE**	**MAE**	**MAPE**
SD1	4280.132	4281.999	4351.690	**3909.353**	**37.188**	**0.225**
SD2	**4258.316**	**4259.165**	**4305.881**	5335.746	41.948	0.227
SDWS	4713.311	4713.471	4733.130	14474.359	73.161	0.417
SS	4298.022	4298.129	4313.878	5927.632	43.523	0.232

Table 4: AIC, AICc, BIC, and loss functions (forecasting window: 14 days)

Model	AIC	AICc	BIC	MSE	MAE	MAPE
SD1	4249.468	4251.349	4320.880	**14365.77**	**61.953**	**0.340**
SD2	**4196.611**	**4197.475**	**4243.972**	22533.51	74.646	0.348
SDWS	4642.673	4642.836	4662.407	41193.64	109.529	0.568
SS	4236.084	4236.192	4251.871	32032.90	84.559	0.383

Table 5: AIC, AICc, BIC, and loss functions (forecasting window: 28 days)

Model	AIC	AICc	BIC	MSE	MAE	MAPE
SD1	4186.649	4188.560	4257.766	**138410.9**	**140.267**	**0.754**
SD2	**4060.468**	**4061.370**	**4107.371**	214083.7	192.565	0.814
SDWS	4486.913	4487.083	4506.456	508463.8	264.977	1.252
SS	4099.487	4099.600	4115.121	929847.5	329.825	1.387

4 Discussion

The paper by (Contreras-Espinoza et al., 2023) identifies score-driven models with weekly seasonal effects for the negative binomial distribution (SD1 and SD2) as providing the most accurate forecasts for COVID-19 cases, outperforming score-driven models without seasonal components (SDWS) and nonlinear state-space models with unobserved components (SS). It introduces the novel application of weekly seasonality components and the use of the negative binomial distribution for COVID-19 data. Additionally, the study emphasizes the potential of these models for forecasting pandemic cases in other geographical and socio-cultural contexts beyond Latin America. This seems reasonable given that the use of the COVID-19 cases from the Bologna WWTP service area confirmed the robustness of their approach, even though the forecasting quality is significantly lower than the ones reported in the article for all the models.

Nevertheless, the study by (Contreras-Espinoza et al., 2023) also has several limitations. First, it lacks details on how the computations are performed, such as the software and libraries used, which limits the reproducibility of the analysis. Second, no estimate for the dispersion parameter of the negative binomial (ν) is reported for the SS model. The authors might have assumed a fixed dispersion parameter based on previous literature or preliminary analyses, thereby simplifying the model. However, such a choice is not described in the paper, limiting again the reproducibility of the study. Third, the reliance on the negative binomial distribution may not capture all aspects of COVID-19 case distributions, suggesting a need for exploring alternative score-driven discrete probability distributions. Fourth, the authors suggest that these models can inform public health decisions, such as implementing quarantines and organizing vaccination processes, thus aiding authorities in managing current and future pandemics. However, the studied models turned out to be not suitable for long-term predictions, which are often more useful in pandemic analysis. Fifth, data limitations due to inconsistent and inaccurate COVID-19 reporting in many Latin American countries could undermine the reliability of the forecasts (Leiva et al., 2023).

5 Conclusions

In this project, score-driven and state-space described in (Contreras-Espinoza et al., 2023) have been applied to daily COVID-19 data referred to the Bologna WWTP service area, from October 13, 2021, to April 4, 2023. Score-driven models with weakly seasonal components for the negative binomial distribution (SD1 and SD2) provided the most accurate forecasts compared to other models, including nonlinear state-space models with unobserved components. However, the forecasting quality was lower than the ones obtained by (Contreras-Espinoza et al., 2023) with COVID-19 data from nine Latin American countries. This suggests that while score-driven models are robust, their performance can vary depending on the dataset's characteristics and quality. In addition, the paper lacks some critical details regarding the software and libraries used, and the estimation of the model parameters, which limits the reproducibility of the analysis. Further research and more comprehensive data are needed to refine these models and improve their generalizability and reproducibility.

References

1. Blasques, F., Koopman, S. J., Łasak, K., & Lucas, A. (2016). In-sample confidence bands and out-of-sample forecast bands for time-varying parameters in observation-driven models. *International Journal of Forecasting*, *32*(3), 875–887. doi:10.1016/j.ijforecast.2015.11.018

2. Caivano, M., Harvey, A., & Luati, A. (2016). Robust time series models with trend and seasonal components. *SERIEs: Journal of the Spanish Economic Association*, *7*(1), 99–120. doi:10.1007/s13209-015-0134-1

3. Commandeur, J.J., & Koopman, S.J. (2007) *An Introduction to State Space Time Series Analysis*. ISBN: 978-0-19-922887-4

4. Contreras-Espinoza, S., Novoa-Muñoz, F., Blazsek, S., Vidal, P., & Caamaño-Carrillo, C. (2022). COVID-19 active case forecasts in Latin American countries using score-driven models. *Mathematics*, *11*(1), 136. doi: 10.3390/math11010136

5. Creal, D., Koopman, S. J., & Lucas, A. (2013). Generalized autoregressive score models with applications. *Journal of Applied Econometrics (Chichester, England)*, *28*(5), 777–795. doi:10.1002/jae.1279

6. Dickey, D. A., & Fuller, W. A. (1979). Distribution of the estimators for autoregressive time series with a unit root. *Journal of the American Statistical Association*, *74*(366), 427. doi:10.2307/2286348

7. Harvey, A., & Kattuman, P. (2020). Time series models based on growth curves with applications to forecasting Coronavirus. *Special Issue 1 - COVID-19: Unprecedented Challenges and Chances*. doi: 10.1162/99608f92.828f40de

8. Harvey, A., & Lit, R. (2020) Coronavirus and the Score-Driven Negative Binomial Distribution. Time Series Lab—Article Series. Available online: https://www.timeserieslab.com/articles/negbin.pdf (Last accessed June 24, 2024).

9. Harvey, A., & Luati, A. (2014). Filtering with heavy tails. *Journal of the American Statistical Association*, *109*(507), 1112–1122. doi:10.1080/01621459.2014.887011

10. Harvey, A. C. (1990). *Forecasting, structural time series models and the Kalman filter*. Cambridge University Press. doi:10.1017/cbo9781107049994

11. Harvey, A. C. (2013). *Dynamic models for volatility and heavy tails: With applications to financial and economic time series (Econometric society monographs)*. Cambridge University Press. doi:10.1017/cbo9781139540933

12. Harvey, A. C., & Shephard, N. (1993). Structural time series models. In: *Handbook of Statistics* (pp. 261–302). Econometrics. doi:10.1016/s0169-7161(05)80045-8

13. Helske, J., Helske, M.J., & Suggests, M.A. (2021). CRAN Package KFAS. Available online: https://cran.r-project.org/web/packages/KFAS/index.html (Last accessed June 24, 2024).

14. Jarque, C. M., & Bera, A. K. (1980). Efficient tests for normality, homoscedasticity and serial independence of regression residuals. *Economics Letters*, *6*(3), 255–259. doi:10.1016/0165-1765(80)90024-5

15. Leiva, V., Alcudia, E., Montano, J., & Castro, C. (2023). An Epidemiological Analysis for Assessing and Evaluating COVID-19 Based on Data Analytics in Latin American Countries. *Biology*, *12*(6), 887. doi: 10.3390/biology12060887